Optimal Conditions for Accelerated Imaging of Fractional Ventilation with Hyperpolarized Gas MRI

Kiarash Emami[1], Yinan Xu[1], Hooman Hamedani[1], Harrilla Profka[1], Yi Xin[1], Puttisarn Mongkolwisetwara[1], Stephen J. Kadlecek[1], Masaru Ishii[2], and Rahim R. Rizi[1]
[1]*Radiology, University of Pennsylvania, Philadelphia, PA, United States,* [2]*Otolaryngology - Head and Neck Surgery, Johns Hopkins University, Baltimore, MD, United States*

INTRODUCTION: Pulmonary ventilation is an important marker in obstructive lung diseases, and its non-invasive imaging can provide useful information to investigate the severity of lung diseases and their response to intervention. Hyperpolarized gas MRI provides a noninvasive platform to directly image distribution of respiratory gas at a high resolution. However quantitative imaging of ventilation still remains as one of the least developed areas using this imaging modality. An improved technique for fractional ventilation (r) imaging was developed by authors [1] based on earlier work of Deninger, *et al.* [2], and was further adapted to large species (with pulmonary volumes comparable to humans) using accelerated imaging [3]. This work investigates optimal conditions for performing such measurements using parallel accelerated imaging.

METHODS: The multi-slice fractional ventilation imaging sequence is shown in **Figure 1**, for the case of three slices. Accelerated imaging was performed using parallel MRI and image reconstruction was done using the well-established GRAPPA methods [4] with a phased array receive coil. Fractional ventilation, r, defined as the ratio of the inspired gas volume to the total end-inspiratory volume, was measured on a regional basis using the technique described earlier [1], by fitting the signal buildup in breaths 1–N to a dynamic recursive model. For simulations, a representative 2D 64×64 image of the middle slice of a pig lung was used as the reference spin density map, $M_S(x,y)$ and $M_A(0)$=0. The corresponding $r(x,y)$ map, derived from the same pig study, was used as the *a priori* r map. Using α=5° and P_AO_2=140mbar throughout, a series of synthetic spin density maps were generated corresponding to a multi-slice ventilation imaging experiment using typical parameters in a pig study. Cartesian k-space acquisition scheme was then simulated according to the equation on the right; $B_c(x,y)$: sensitivity profile for c-th coil; N_{PE}: number of RF pulses. Various levels of complex random noise was added to the k-space signal. The spin density at each time point was sampled using a 1×4 phased array coil with identical sinusoidal sensitivity profile. The accelerated acquisitions were performed using ACL=8–32 and AR=2–4. Images from coils were reconstructed using GRAPPA algorithm and combined to obtain a single image for the corresponding time point, as shown in **Figure 2**. The *effective* acceleration factor of $64/N_{PE}$ is calculated according to a given pair of ACL and AR: N_{PE}=ACL+(64−ACL)/AR pulses. The resulting images was then fit to the fractional ventilation model to yield maps of α and r. Results were evaluated by: (*i*) RMS difference between the estimated and reference r maps, and (*ii*) correlation coefficient R for the voxel-by-voxel linear regression between the two maps.

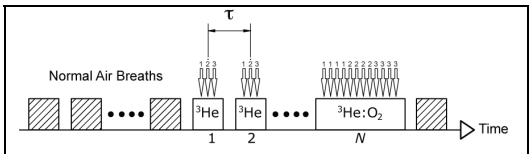

Figure 1. Multi-slice fractional ventilation imaging sequence. NS images are acquired during each end-inspiratory HP gas breath-hold (NS=3 shown here). A long breath-hold is performed after inhaling the last HP gas breath, during which the flip angle mapping sequence is performed (n=4 shown here). Arrows (⇩) indicate image acquisition per slice. The dashed and blank boxes represent air and HP gas breaths (N shown here), respectively.

$$S_c(k_x,k_y)=\sum_{x=1}^{N_{PE}}\sum_{y=1}^{N_{PE}} M_A(x,y)\cdot B_c(x,y)\cdot\sin\alpha\cdot\cos^{k_x-1}\alpha\cdot\exp\left[-(k_x-1)\mathrm{TR}\cdot P_AO_2/\xi\right]\cdot\exp\left[j2\pi(k_x+k_y)/N_{PE}\right]$$

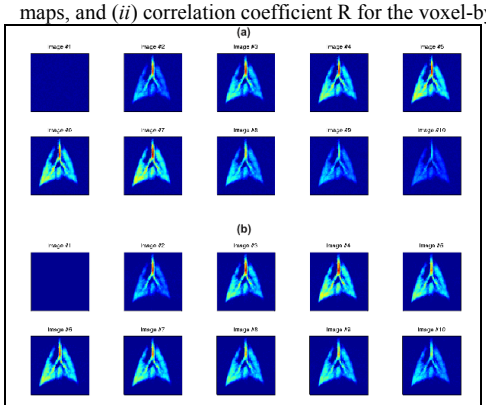

Figure 2. Combined images of signal intensity evolution in the synthetic pig lung over the course of the simulated fractional ventilation imaging experiment: **(a)** with and **(b)** without acceleration. Note the larger residual signal at the end of the undersampled image acquisition sequence.

RESULTS: r estimation error as a function of the applied α value was initially evaluated in a single imaged voxel used to determine the optimal flip angle over a range of N_{PE}=24–64. The minimum error interval gets smaller for larger N_{PE} as a result of the more pronounced effect of RF-induced depolarization. Optimal flip angle, α_{opt} (α that minimizes Δr) showed a highly linear behavior with respect to N_{PE} (R=0.98–0.99 for r=0.2–0.4) and is confined to the range α_{opt}=5–7° for N_{PE}=24–64. The variation of RMS error in the computed 64×64 r maps is plotted was evaluated as a function of α, with the error normalized with respect to the minimum error (i.e. the optimal undersampling condition). $\Delta r_2/\Delta r_{2,min}$ and R (linear regression between *a priori* and estimated r maps) both reach a local minimum and maximum, respectively, as a function of α (not shown for brevity). Based on the RMS error, r estimation error reaches a global minimum around N_{PE}≈31, beyond which the trend reverses, as shown in **Figure 3**, and increases with further undersampling. The nominal optimal scan parameters for this case are ACL=24 and AR=5, corresponding to an effective acceleration factor of ~2×. A similar behavior is observed based on the correlation coefficient of r maps. The technique was successfully implemented in pigs under mechanical ventilation as reported earlier [3]. A representative set of results is shown in **Figure 4**.

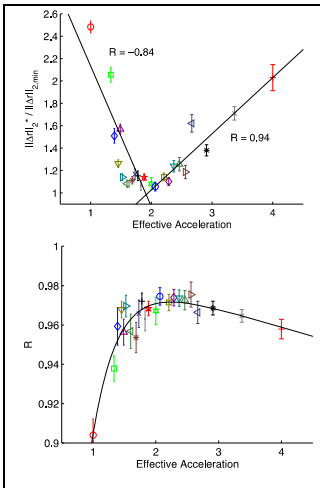

Figure 3. Variation of normalized RMS error and correlation coefficient between the calculated and *a priori* r maps as a function of effective acceleration ratio. Error bars represent the StdDev over ~50 iterations.

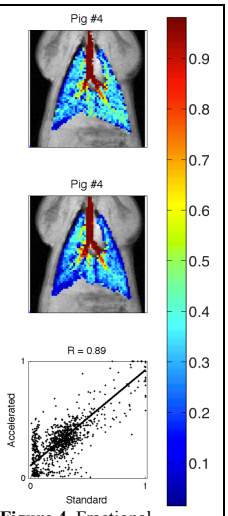

Figure 4. Fractional ventilation maps acquired in a pig lung with and without image acceleration agree well with each other.

DISCUSSION AND CONCLUSION: In contrast to the single imaging voxel, it is evident that undersampling cannot indefinitely improve r accuracy, and there is a limit beyond which the information loss due to undersampling (e.g. reconstruction artifacts) outweighs the gain in reducing RF pulses and acquisition time. For assessment of accuracy of accelerated ventilation imaging, the normalized RMS error $\Delta r_2/\Delta r_{2,min}$, not only reflects the effect of the number of RF pulses and noise, but also incorporates the inaccuracy introduced by undersampled image reconstruction artifacts. The minimum error condition for each (ACL,AR) pair also represents the corresponding optimal flip angle, α_{opt} (not shown for brevity). It should be emphasized that this analysis only pertains to this representative case, and optimality conditions, in general, will be a function of other experimental details, including the number of parallel coils, imaging resolution, and achievable SNR.

Large species, humans included, breathe over a respiratory time scale of a few seconds (typical 4–8 sec breathing cycle at rest). Rodents have a respiratory rate of up to 10 times faster. The slower breathing rate of larger species means that certain signal decay mechanisms will longer be negligible in HP gas ventilation signal buildup. (e.g. the oxygen depolarization effect ($T_{1,\ in\ vivo}$ ≈ 18 s) induces a more prominent signal attenuation over the experimental time scale). Therefore in addition to diminishing the RF effect in r estimation, acceleration shortens the breath-hold time necessary to acquire the images, thereby reducing the overall time and the associated O2-induced decay.

REFERENCES: [1] Emami K *et al.*, Magn Reson Med. 2010 Jan; 63(1):137-50. [2] Deninger AJ *et al.*, *Magn Reson Med*. 2002 Aug; 48(2):223-32. [3] Emami K *et al.*, Proc 19th ISMRM 2011 May. [4] Griswold MA *et al.*, Magn Reson Med. 2002 Jun;47(6):1202-10.